Applied Chemical Engineering (2021) Volume 4 Issue 2
doi:10.24294/ace.v4i2.1345

Original Research Article

Effect of doping with different amounts of nickel on the selective catalytic reduction NO of manganese oxides

Liqiang Chen[1,2], Lina Sun[1,2], Mingxia Zhu[1], Lihua Chen[1], Hao Li[1,2], Donghui Hu[1,2], Lihong Liu[1,2], Fulong Yuan[2*]

[1] *School of Science, Heihe University, Heihe 164300, Heilongjiang, China*

[2] *School of Chemistry, Chemical Engineering and Materials, Heilongjiang University, Harbin 150080, China. E-mail: yflhlj@163.com*

ABSTRACT

Nickel-manganese oxides were studied for selective catalytic reduction of NO by XRD, H_2-TPR and N_2 adsorption-desorption. The study was found that the catalyst $Ni_{0.4}Mn_{0.6}O_x$ showed the best SCR activity, the reasons may be as follows: $Ni_{0.4}Mn_{0.6}O_x$ catalyst showed the optimal synergistic effect between nickel and manganese and appropriate redox ability, which were conducive to NH_3 under the condition of low temperature catalytic reduction of NO.

Keywords: Selective Catalytic Reduction; NO; Nickel-Manganese Oxides; Synergistic Effect

ARTICLE INFO

Received: 3 June 2021
Accepted: 20 July 2021
Available online: 27 July 2021

1. Introduction

NO_x is one of the main components of current atmospheric environmental pollutants. Excessive NO_x will lead to a series of environmental problems, such as acid rain, haze, photochemical smog and heat island effect, which is very harmful to human health, animals and plants[1]. Scientists from various countries have been focusing on NO_x elimination research in recent decades. The fixed source industrial flue gas denitration technology is mainly ammonia selective catalytic reduction of NO_x (NH_3-SCR). At present, the commercial denitration catalyst for fixed source NH_3-SCR method is $V_2O_5(WO_3)/TiO_2$, which has the following problems: V_2O_5 has biological toxicity, narrow operating temperature window (300–400 ℃), low selectivity and poor thermal stability at high temperature[2–4].

As the standards for the total emission and emission concentration of NO_x and SO_2 become more and more strict, desulfurization is generally required before denitration in order to meet their emission standards at the same time. After desulfurization, the flue gas temperature of thermal power generation is usually lower than 300 ℃. According to statistics, the flue gas temperature of boilers such as self-provided power station boilers, coal-fired, oil and gas boilers, glass furnaces, waste incinerators, cement furnaces, petrochemical cracking furnaces, coking furnaces, chemical plants, metallurgical sintering furnaces, electronics, new energy and metallurgy is usually 120–300 ℃. Therefore, the mature fixed source nh3-scr denitration catalyst is difficult to be applied to

the purification of exhaust gas after desulfurization. In this context, the development of low-temperature nh3-scr denitration catalyst is an inevitable way to solve the problem of low-temperature flue gas discharged by the above boilers[5].

Since the valence electron layer structure of Mn is $3d^5 4s^2$, it has more variable valence states than transition metals such as SM, Cr, Cu, Fe, CE, W and Nb. Especially at low temperature, the oxidation states of Mn can transform each other, which is one of the main reasons for its excellent low-temperature SCR catalytic activity[6].

At present, there are many reports on Mn-based catalysts, such as MnO_x and Mn-based composite oxides[7]. Mn-based composite oxides mainly include the following types: SM–Mn[8], Fe–Mn[9–11], CE–Mn[12], EU–Mn[13], Co–Mn[14], Mn–Ti[15], Mn–W[16] and Ni–Mn[17,18]. These catalysts have excellent low-temperature SCR performance. This paper synthesized a series of catalysts $Ni_yMn_{1y}O_x$ (y = 0.1–0.5) with sol-gel method and studied the effect of different nickel doping on NH_3-SCR denitration activity of manganese oxides by means of X-ray diffraction (XRD), temperature programmed reduction (H_2-TPR) and specific surface area (BET).

2. Experimental part

2.1 Preparation of catalyst

Mn doped $Ni_yMn_{1-y}O_x$ (y = 0.1–0.5) with different Ni content was prepared by sol-gel method, y = Ni/(Ni + Mn). Accurately weigh a certain amount of nickel nitrate and manganese nitrate according to the stoichiometric ratio to ensure that the total mass of nickel nitrate and manganese nitrate is 0.010 mol. At the same time, measure 30 mL of ethanol, 30 mL of glacial acetic acid and 10 mL of deionized water, add the above nitrate to the mixed solution, and stir at room temperature for 5 hours. After that, the mixed solution was placed in a 30 degree oven for 6 D, and the dried gels were dried in the oven at 110 degrees for the night. The calcination conditions of catalyst precursor are as follows: raise the temperature from room temperature to 500 ℃ at the heating rate of 5 ℃/min and keep it for 6 hours, then cool it naturally to room temperature, grind and tablet it, and then granulate it. Take 40–60 mesh catalyst for NH_3-SCR activity test.

2.2 Evaluation of the catalyst

2.2.1 Activity test

In order to simulate the real denitration atmosphere, four gas channels are connected. The first gas is 0.8% NO/N_2 of 25 mL, the second gas is 0.8% NH_3/N_2 of 25 mL, the third gas is 50% NO/N_2 of 12 ml, and the fourth gas is 138 ml of high-purity N_2 as equilibrium gas. The concentration of each gas in the whole mixture is 0.1% NO, 0.1% NH_3 and 3% O_2. The volume of catalyst is 0.3 mL, the particle size is 40–60 mesh, the outer diameter of quartz tube is 8 mm, the inner diameter is 6 mm, and the tube length is 50 cm. NO_2, N_2O, NO and NH_3 were analyzed online by NO_x and ammonia analyzer (ECO physics, Switzerland), and the data after each temperature point was stable for 1 h were collected.

2.2.2 Characterization of the catalyst

2.2.2.1 Characterization of XRD

The samples were determined by wide-angle XRD with D/MAX-3B (40 kV, 200 MA) instrument produced by Japan science company. The conditions are as follows: Cu Target Ka line (λ = 0.15406 nm), 2θ's scanning range is 5°–80°, the sampling step size is 0.02°, the scanning speed is 10°/min, DS = 1°, SS = 1°, and RS = 0.3°.

2.2.2.2 Adsorption-desorption characterization of N_2

The N_2 adsorption-desorption isotherm of the sample was measured on Tristar 3020 automatic specific surface area and pore size analyzer produced by instrument company. Before the test, the sample shall be degassed in vacuum at 150 ℃ for 8 h, and then the N_2 adsorption desorption isothermal curve of the sample shall be measured at –196℃.

2.2.2.3 Test of H_2—TPR

The characterization of hydrogen temperature programmed reduction catalyst can obtain some in-

formation about the redox properties and surface of the catalyst. In this paper, the H_2-TPR of catalyst was determined by Xianquan tp-5080 adsorption instrument. The operation steps are as follows: 1) weigh 0.020 g catalyst powder and fix it in a quartz tube with quartz cotton; 2) add pure O_2 with a flow rate of 30 mL/min, and raise the temperature from room temperature to 300 ℃ at a heating rate of 10 ℃/min and keep it for 1 h; 3) cool down to room temperature in pure O_2 atmosphere of 30 mL/min, and switch the pure O_2 atmosphere to 5% H_2/N_2 atmosphere, and the flow remains at 30 ml/min; 4) after the baseline is stable, increase the temperature from room temperature to 900 ℃ at a heating rate of 10 ℃/min.

3. Results and discussions

3.1 Effect of nickel doping on catalytic performance

The SCR denitration performance of the catalyst $Ni_yMn_{1-y}O_x$ (y = 0.1–0.5) was investigated. The results are shown in **Figure 1**. It can be seen from **Figure 1(a)** that the NO conversion of pure MnO_x is 53% at 90 ℃, while the NO conversion of Ni-doped catalyst $Ni_yMn_{1-y}O_x$ (y = 0.1–0.5) reaches more than 90% at 90 ℃. The NO conversion of pure MnO_x at 110 ℃ is 76%, while the NO conversion of Ni-doped series catalysts $Ni_yMn_{1-y}O_x$ (y = 0.1–0.5) is 100%, which shows that Ni doping can effectively improve the NO conversion of manganese oxides at low temperature rate. The operating temperature window of series catalyst $Ni_yMn_{1-y}O_x$ (y = 0.1–0.5) is 90–270 ℃, and the NO conversion is more than 90%, while the operating temperature window of pure MnO_x is only 130–210 ℃. This shows that Ni doping is beneficial to broaden the operating temperature window of $Ni_yMn_{1-y}O_x$ (y = 0.1–0.5) oxide. At 210–360 ℃, the series catalysts $Ni_yMn_{1-y}O_x$ (y = 0.1–0.5) have higher no elimination rate than pure MnO_x.

As can be seen from **Figure 1(b)**, the N_2 selectivity of series catalysts $Ni_yMn_{1-y}O_x$ (y = 0–0.5) decreases with the increase of temperature at 110–360 ℃. At 150 ℃, the N_2 selectivity of pure MnO_x is only 49%. The N_2 selectivity of catalysts $Ni_{0.1}Mn_{0.9}O_x$, $Ni_{0.2}Mn_{0.8}O_x$ and $Ni_{0.3}Mn_{0.7}O_x$ is about 50% at 170, 190 and 210 ℃, respectively, while the N_2 selectivity of catalysts $Ni_{0.4}Mn_{0.6}O_x$ and $Ni_{0.5}Mn_{0.5}O_x$ is still more than 50% at 360 ℃. The catalyst $Ni_{0.4}Mn_{0.6}O_x$ showed slightly better N_2 selectivity than $Ni_{0.5}Mn_{0.5}O_x$ at 190–360 ℃. This shows that Ni doping is beneficial to improve the N_2 selectivity of $Ni_yMn_{1-y}O_x$ (y = 0–0.5) oxide, and the N_2 selectivity increases with the increase of Ni doping. When the molar ratio of Ni/(Mn + Ni) reaches 0.4, the N_2 selectivity is the best.

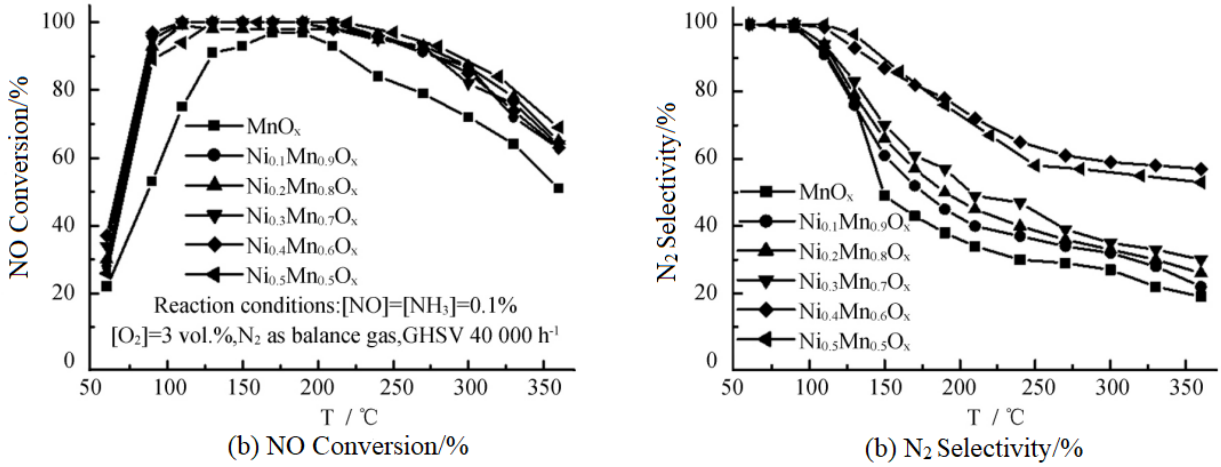

Figure 1. SCR activity of $Ni_yMn_{1-y}O_x$ catalyst with different molar ratios of Ni/(Mn + Ni).

3.2 Analysis of XRD

A series of catalysts $Ni_yMn_{1-y}O_x$ (y = 0.1–0.5) were characterized by XRD. The results are shown in **Figure 2**. It can be seen from **Figure 2** that the diffraction peak of pure MnO_x sample belongs to crystalline Mn_2O_3, but the diffraction peak is relatively

weak (PDF card 24-0508), which indicates that there is a considerable amount of amorphous manganese oxide in the sample. The sample $Ni_{0.1}Mn_{0.9}O_x$ has the diffraction peak of $NiMn_2O_4$ at 18.14°, 35.87° and 43.21° respectively, and the diffraction peak of Mn_2O_3 at 8.70°, 32.65° and the intensity of the diffraction peak is weak. This shows that the sample is miscible and contains oxides of $NiMn_2O_4$, Mn_2O_3 and amorphous manganese. When the molar ratio of Ni/(Ni + Mn) is 0.2, a series of Mn_2O_3 diffraction peaks at 28.88°, 32.56°, 38.18°, 55.24° disappear, and a series of $NiMn_2O_4$ (PDF card 01-1110) diffraction peaks appear at the same time. The degree is the strongest when the molar ratio of Ni/(Ni + Mn) is 0.3. Then it decreases with the further increase of Ni doping. When the molar ratio of Ni/(Ni + Mn) is 0.5, the diffraction peak of NiO appears at 75.45°. This shows that when the molar ratio of Ni/(Ni + Mn) is ≤ 0.4, there will be no diffraction peak of nickel oxide, and nickel and manganese mainly exist as bimetallic oxides, which is conducive to the interaction between nickel and manganese.

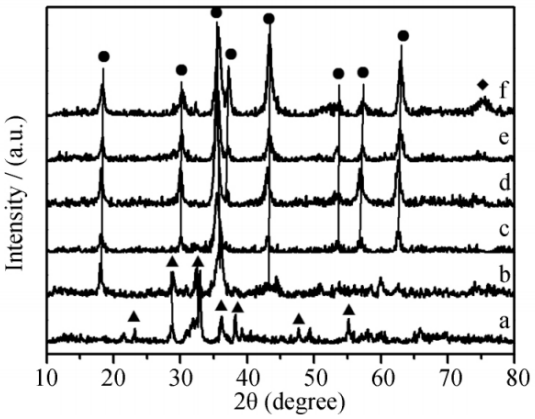

(a) MnO_x, (b) $Ni_{0.1}Mn_{0.9}O_x$, (c) $Ni_{0.2}Mn_{0.8}O_x$, (d) $Ni_{0.3}Mn_{0.7}O_x$, (e) $Ni_{0.4}Mn_{0.6}O_x$, (f) $Ni_{0.5}Mn_{0.5}O_x$ (◆NiO, ▲Mn_2O_3 and ●$NiMn_2O_4$).

Figure 2. XRD pattern of $Ni_yMn_{1-y}O_x$ catalyst with different molar ratios of Ni/(Mn + Ni).

3.3 Analysis of specific surface area and pore structure characteristics

See **Table 1** for the specific surface area and pore structure characteristics of catalyst $Ni_yMn_{1-y}O_x$. It can be seen from **Table 1** that the specific surface area of $Ni_yMn_{1-y}O_x$ (y = 0.1–0.5) is larger than that of MnO_x and NiO_x (23.1 and 31.3 m^2/g), which indicates that Ni doping into MnO_x can significantly increase the specific surface area of $Ni_yMn_{1-y}O_x$ (y = 0.1–0.5), and the specific surface area of catalyst $Ni_yMn_{1-y}O_x$ (y = 0.1–0.4) is less affected by Ni/(Ni + Mn) ratio. With the increase of Ni/(Mn + Ni) ratio to 0.3, the pore volume of catalyst $Ni_yMn_{1-y}O_x$ (y = 0.1–0.5) increased from 18.8 × 10^{-2} cm^3/g monotonically increased to 20.2 × 10^{-2} cm^3/g. By further increasing the Ni/(Ni + Mn) ratio to 0.5, the pore volume of catalyst $Ni_{0.5}Mn_{0.5}O_x$ decreased to 15.2 × 10^{-2} cm^3/g. With the increase of Ni/(Mn + Ni) ratio, the average pore size of catalyst $Ni_yMn_{1-y}O_x$ follows a similar law. The above results show that Ni has physicochemical properties influencing the $Ni_yMn_{1-y}O_x$ (y = 0.1–0.5), attributed to the strong interaction between Mn and Ni.

Table 1. Physicochemical data for $Ni_yMn_{1-y}O_x$ catalysts with different Ni/(Ni + Mn) mole ratios

Sample	Surface area of catalyst/ ($m^2 \cdot g^{-1}$)	Pore volume (10^{-2} $cm^3 \cdot g^{-1}$)	Mean pore size/nm
NiO_x	31.3	6.1	7.8
MnO_x	23.1	11.3	19.6
$Ni_{0.1}Mn_{0.9}O_x$	43.3	18.8	17.4
$Ni_{0.2}Mn_{0.8}O_x$	39.8	19	19.1
$Ni_{0.3}Mn_{0.7}O_x$	41.4	20.2	19.5
$Ni_{0.4}Mn_{0.6}O_x$	43.2	16.7	15.4
$Ni_{0.5}Mn_{05}O_x$	36.9	15.2	14.5

3.4 Analysis of H_2—TPR

In order to study the effect of Ni doping on the redox capacity of catalyst $Ni_xMn_{1-x}Ti_{10}$, the catalyst $Ni_xMn_{1-x}Ti_{10}$ was characterized by H_2-TPR. The results are shown in **Figure 3**. There are two reduction peaks of MnO_x at 586 K and 708 K, corresponding to the reduction of $MnO_2 \rightarrow Mn_3O_4$ and $Mn_3O_4 \rightarrow MnO$ respectively, which is consistent with literature[19]. Due to its large negative reduction potential, MnO cannot be further reduced to metal Mn at less than 1073 K, which has been reported by many studies. The peak of sample $Ni_yMn_{1-y}O_x$ (y = 0.1–0.5) at 503–533 K corresponds to the reduction of $MnO_2 \rightarrow Mn_3O_4$. When Ni/(Ni + Mn) ratio is 0.2, the reduction temperature is the highest, but with the further increase of Ni/(Ni + Mn) ratio, the reduction

temperature moves to low temperature, indicating that there is an interaction between Ni and Mn, making the reduction of $MnO_2 \rightarrow Mn_3O_4$ easier. The reduction peak of sample $Ni_yMn_{1-y}O_x$ (y = 0.1–0.5) at 600–708 K also moves to low temperature with the increase of Ni/(Ni + Mn) ratio. For the samples with Ni/(Ni + Mn) ratio of 0.1, 0.2 and 0.3, the second reduction peak includes reduction of $Mn_3O_4 \rightarrow MnO$ and $Ni^{2+} \rightarrow Ni^0$.

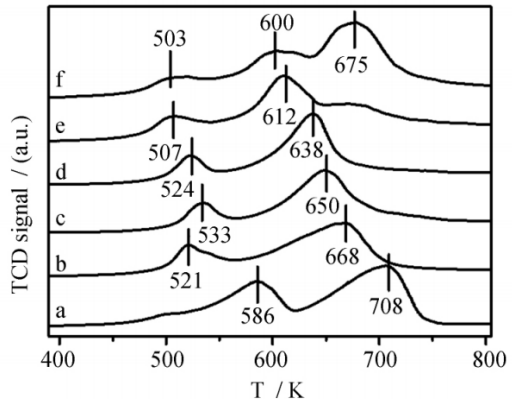

(a) MnO_x, (b) $Ni_{0.1}Mn_{0.9}O_x$, (c) $Ni_{0.2}Mn_{0.8}O_x$, (d) $Ni_{0.3}Mn_{0.7}O_x$, (e) $Ni_{0.4}Mn_{0.6}O_x$, (f) $Ni_{0.5}Mn_{0.5}O_x$

Figure 3. H_2–TPR pattern of $Ni_xMn_{1-x}Ti_{10}$ catalysts.

For the samples with Ni/(Ni + Mn) ratio of 0.4 and 0.5, the third reduction peak appears at 686 K and 675 K respectively, and the peak area increases with the increase of Ni, which belongs to the reduction of $Ni^{2+} \rightarrow Ni^0$. The first reduction peak moves towards low temperature, which can be inferred that the reduction ability at low temperature is improved due to Ni doping. This may be an important reason for the excellent low-temperature NH_3-SCR activity of these modified catalysts. The excellent low temperature NH_3-SCR activity may be related to $Mn^{4+} \rightarrow Mn^{3+}$reduction. Ni is not the active metal of low temperature NH_3-SCR reaction, which is not discussed here. It is well known that the reduction temperature and hydrogen consumption mainly determine the redox capacity of the catalyst. Therefore, it can be seen from the H_2-TPR analysis results that $Ni_{0.4}Mn_{0.6}O_x$ has appropriate redox capacity. The author's previous research results show that the high redox capacity of Ni Mn spinel can over oxidize NH_3 to N_2O, NO and NO_2, resulting in low N_2 selectivity in the medium temperature region[20]. Therefore, appropriate redox capacity is conducive to the excellent no conversion and N_2 selectivity of the catalyst in the medium temperature region.

4. Conclusions

The selective catalytic reduction of no by NH_3 over $Ni_yMn_{1-y}O_x$ (y = 0.1–0.5) catalysts doped with different amounts of Ni was studied in this paper. The results show that the catalytic activity of $Ni_{0.4}Mn_{0.6}O_x$ is the best. The possible reason is that when the molar ratio of Ni/(Mn + Ni) reaches 0.4, the interaction between nickel and manganese is the best and suitable redox capacity, which are conducive to the selective catalytic reduction of no by NH_3 at low temperature.

Conflict of interest

The authors declare that they have no conflict of interest.

Acknowledgements

This article was supported by special project for scientific research talents of Heilongjiang Provincial Department of Education (18kyywfrc01); the project was supported by Heilongjiang Natural Science Youth Fund (qc2018012).

References

1. Elbouazzaoui S, Corbos EC, Courtois X, *et al.* A study of the deactivation by sulfur and regeneration of a model NSR $Pt/Ba/Al_2O_3$ catalyst. Applied Catalysis B, Environmental 2005; 61: 236–243.
2. Huang Z, Liu Z, Zhang X, *et al.* Inhibition effect of H_2O on V_2O_5/AC catalyst for catalytic reduction of NO with NH_3 at low temperature. Applied Catalysis B, Environmental 2006; 63: 260–265.
3. Larrubia MA, Ramis G, Buse G. An FT-IR study of the adsorption of urea and ammonia over V_2O_5-MoO_3 urea and ammonia over V_2O_5-MoO_3-TiO_2 SCR catalysts. Applied Catalysis B, Environmental 2000; 27: 145–151.
4. Reddy BM, Rao KN, Reddy GK, *et al.* Characteri-

zation and catalytic activity of V_2O_5/Al_2O_3-TiO_2 for selective oxidation of 4-methylanisole. Journal of Molecular Catalysis A 2006; 253: 44–51.
5. Chen L, Sun J, Liu L, *et al.* Calcination temperature on the catalytic reduction NO activity of nickel-manganese-titanium oxide. Journal of Engineering of Heilongjiang University 2018; 9(2): 33–37.
6. Armor JN. Catalytic solutions to reduce pollutants. Catalysis Today 1997; 38: 163–167.
7. Shi J, Gao C, Liu C, *et al.* Porous MnO_x for low-temperature NH_3-SCR of NO_x: the intrinsic relationship between surface physicochemical property and catalytic activity. Journal of Nanoparticle Research 2017; 19: 194–205.
8. Meng D, Zhan W, Guo Y, *et al.* Highly effective catalyst of Sm-MnO_x for the NH_3-SCR of NO_x at low temperature: promotional role of Smand its catalytic performance. ACS Catalysis 2015; 5: 5973–5983.
9. France LJ, Yang Q, Li W, *et al.* Ceria modified FeMnO$_x$-enhanced performance and sulphur resistance for low-temperature SCR of NO_x. Applied Catalysis B, Environmental 2017; 206: 203–215.
10. Fang N, Guo J, Shu S, *et al.* Enhancement of low-temperature activity and sulfur resistance of $Fe_{0.3}Mn_{0.5}Zr_{0.2}$ catalyst for NO removal by NH_3-SCR. Chemical Engineering Journal 2017; 325: 114–123.
11. Yan L, Liu Y, Zha K, *et al.* Scale-activity relationship of MnO_xFeO_y nanocage catalysts derived from prussian blue analogues for low-temperature NO reduction: experimental and DFT studies. ACS Applied Materials & Interfaces 2017; 9(3): 2581–2593.
12. Gao G, Shi J, Liu C, *et al.* Mn/CeO_2 catalysts for SCR of NO_x with NH_3: Comparative study on the effect of supports onlow-temperature catalytic activity. Applied Surface Science 2017; 411: 338–346.
13. Sun P, Guo R. Liu S, *et al.* The enhanced performance of MnO_x catalyst for NH_3-SCR reaction by the modification with Eu. Applied Catalysis A, General 2017; 531: 129–138.
14. Li Y, Li Y, Shi Q, *et al.* Novel hollow microspheres $Mn_xCo_{3-x}O_4$ (x = 1, 2) with remarkable performance for low-temperature selective catalytic reduction of NO with NH_3. Journal of Sol-Gel Science and Technology 2017; 81: 576–585.
15. Guo R, Li M, Sun P, *et al.* The enhanced resistance to P species of an Mn-Ti catalyst for selective catalytic reduction of NO_x with NH_3 by the modification with Mo. RSC Advances 2017; 7: 19912–19923.
16. Liu F, Shan W, Lian Z. Novel $MnWO_x$ catalyst with remarkable performance for low temperature NH_3-SCR of NO_x. Catalysis Science and Technology 2013; 3(10): 2699–2707.
17. Cai S, Zhang D, Shi L, *et al.* Porous Ni-Mn oxide nanosheets in situ formed on nickel foam as 3D hierarchical monolith de-NO_x catalysts. Nanoscale 2014; 6(13): 7346–7353.
18. Wan Y, Zhao W, Tang Y, *et al.* Ni-Mn bi-metal oxide catalysts for the low temperature SCR removal of NO with NH_3. Applied Catalysis B, Environmental 2014; (148-149)C: 114–122.
19. Lian Z, Liu F, He H. Manganese-niobium mixed oxide catalyst for the selective catalytic reduction of NO_x with NH_3 at low temperatures. Chemical Engineering Journal 2014; 250: 390–398.
20. Chen L, Niu X, Li Z, *et al.* Promoting catalytic performances of Ni-Mn spinel for NH_3-SCR by treatment with SO_2 and H_2O. Catalysis Communications 2016; 85: 48–51.